The full details of the published version of the article are as follows:

TITLE: Excessive growth hormone expression in male GH transgenic mice adversely alters bone architecture and mechanical strength

AUTHORS: S. V. Lim M. Marenzana M. Hopkinson E. O. List J. J. Kopchick M. Pereira B. Javaheri J. P. Roux P. Chavassieux M. Korbonits C. Chenu

JOURNAL TITLE: Endocrinology

PUBLICATION DATE: April 2015

PUBLISHER: Oxford University Press

DOI: 10.1210/en.2014-1572

Excessive Growth Hormone Expression in Male GH Transgenic Mice Adversely Alters Bone Architecture and Mechanical Strength

S. V. Lim, M. Marenzana, M. Hopkinson, E. O. List, J. J. Kopchick, M. Pereira, B. Javaheri, J. P. Roux, P. Chavassieux, M. Korbonits, and C. Chenu

Department of Comparative and Biomedical Sciences (S.V.L., M.H., M.P., B.J., C.C.), Royal Veterinary College, London NW1 0TU, United Kingdom;

Imperial College (M.M.), London SW7 2AZ, United Kingdom;

Edison Biotechnology Institute (E.O.L., J.J.K.), Ohio University, Ohio 45701;

INSERM Unité Mixte de Recherche 1033 and Université de Lyon (J.P.R., P.C.), 69372 Lyon Cedex 08, France;

Department of Endocrinology (M.K.), Barts and the London School of Medicine, Queen Mary University of London, London EC1A 6BQ, United Kingdom

Corresponding author: cchenu@rvc.ac.uk

Abstract

Patients with acromegaly have a higher prevalence of vertebral fractures despite normal bone mineral density (BMD), suggesting that GH overexpression has adverse effects on skeletal architecture and strength. We used giant bovine GH (bGH) transgenic mice to analyze the effects of high serum GH levels on BMD, architecture, and mechanical strength. Five-month-old hemizygous male bGH mice were compared with age- and sex-matched nontransgenic littermates controls (NT; n=16/group). Bone architecture and BMD were analyzed in tibia and lumbar vertebrae using microcomputed tomography. Femora were tested to failure using three-point bending and bone cellular activity determined by bone histomorphometry. bGH transgenic mice displayed significant increases in body weight and bone lengths. bGH tibia showed decreases in trabecular bone volume fraction, thickness, and number compared with NT ones, whereas trabecular pattern factor and structure model index were significantly increased, indicating deterioration in bone structure. Although cortical tissue perimeter was increased in transgenic mice, cortical thickness was reduced. bGH mice showed similar trabecular BMD but reduced trabecular thickness in lumbar vertebra relative to controls. Cortical BMD and thickness were significantly reduced in bGH lumbar vertebra. Mechanical testing of femora confirmed that bGH femora have decreased intrinsic mechanical properties compared with NT ones. Bone turnover is increased in favor of bone resorption in bGH tibia and vertebra compared with controls, and serum PTH levels is also enhanced in bGH mice. These data collectively suggest that high serum GH levels negatively affect bone architecture and quality at multiple skeletal sites.

Introduction

GH is a peptide hormone secreted by the anterior pituitary gland, which has catabolic and anabolic actions on many organ systems. In the skeleton, it facilitates linear bone growth by causing chondrocyte proliferation at the epiphyseal cartilage in the growth plate region (1,–3). GH also has numerous metabolic functions regulating carbohydrate and lipid metabolism (4). It induces intracellular signals through the GH receptor (GHR), a predimerized cytokine receptor signaling through the Janus kinase (JAK)-signal transducer and activator of transcription pathway (STAT) (5). Many of the growth-promoting actions of GH are mediated by IGF-1, which is synthesized in most peripheral tissues, with liver synthesis contributing primarily to circulating IGF-1 levels (1). Both GH and IGF-1 are anabolic hormones for the skeleton and are involved in the stimulation of bone formation (1, 6). Although they have overlapping effects, GH and IGF-1 also have distinct effects on skeletal development, bone growth, and fracture risk (7).

The importance of GH in the regulation of bone growth is best seen in patients with GH deficiency (GHD) or GH excess (8, 9). Patients with GHD have a low bone turnover, whereas excess GH, usually due to a GH-secreting pituitary tumor causing acromegaly, is associated with increased bone turnover (9, 10). Although patients with acromegaly have characteristically enlarged bones and excess cortical bone and osteophytes, clinical reports and experimental studies have shown inconsistent data on bone mineral density (BMD) and, paradoxically, a number of studies suggested increased fracture risk in these patients (11,–16). The clinical picture regarding bone is complicated by the fact that patients with acromegaly often have hypogonadism due to excess prolactin secretion and/or reduced gonadotropins due to tumor pressure effects. In active acromegaly, high GH levels are associated with increased cortical BMD, whereas the effects on trabecular BMD are more variable (17,–20). In addition, fracture risk in acromegaly was shown to be either associated with BMD or independent of it, suggesting that BMD alone is not a sufficient indicator of fracture risk (12,–14, 21). The effects of an excess GH on bone architecture and strength are still unclear. Bone fracture risk is dependent on the overall bone strength, which itself depends on bone structural and material properties, both of which are affected by bone turnover (22). Structural properties of bone include its geometry and architecture (23), whereas its material properties depend mainly on bone mineral and collagen contents that are affected by the rate of bone remodeling (24).

Several transgenic animal models have been developed to study the effects of GH on bone. Transgenic expression of bovine GH (bGH) or rat GH in mice is now commonly used to study GH physiology, and GH is often fused with a transcriptional regulatory element such as the

metallothionein promoter/enhancer whose expression is constitutive (25,–27). Also, supraphysiological levels of GH are usually found in these GH transgenic mice (25). Although several studies have shown changes in bone growth, turnover and BMD in transgenic mice overexpressing GH (26, 28,–30), there has been no extensive characterization of the three-dimensional bone microarchitecture in cortical and trabecular compartments in relation with bone strength in those mice.

The aim of this study was to examine whether the observed higher prevalence of vertebral fractures in acromegaly patients (11,–15) could be explained by a compromised bone architecture and strength. We used giant bGH transgenic mice to examine the effects of high serum GH and IGF-1 levels on BMD, on vertebra and tibia trabecular, and cortical bone architecture as well as on mechanical strength in comparison with nontransgenic littermates control mice of the same age and sex. Moreover, this work served to ascertain the potential of this transgenic mouse model for further studies of the skeletal changes associated with acromegaly.

Materials and methods

Animals

bGH transgenic mice and nontransgenic littermates controls (NT) were generated as described by Berryman et al (27). Briefly, bGH transgenic mice were generated using a metallothionein transcriptional regulatory element linked to the first exon and intron of the bGH cDNA. C57BL/6J embryos were injected with this construct, and the mice were maintained in the genetic background. In our study, we used 5-month-old male mice and a total of 16 mice for each genotype (NT and bGH) were analyzed. Blood was collected immediately after killing for hormone measurements. The left tibiae and femora as well as lumbar vertebrae of 16 mice/group were dissected, fixed in 10% neural-buffered formalin for 24–72 hours, and stored in 70% ethanol at 4°C for microcomputed tomography (micro-CT) analysis of BMD and bone architecture. Right femora were dissected and stored at −20°C for mechanical testing. To label bone-forming surfaces in trabecular bone, mice (nine per group) were injected ip with calcein (Sigma-Aldrich) on day 8 and alizarin red complexone (Sigma-Aldrich) on day 3, prior to euthanasia. Right tibiae and L4 vertebrae were collected from these mice for bone histomorphometry analysis.

Micro-CT analysis of tibiae and vertebrae

Tibiae were scanned using high resolution (5 µm pixel size) micro-CT (Skyscan 1172) at x-ray energy settings of 50 kV and 200 µA, using a 0.5 mm aluminum filter. Skyscan software was used for computed tomography reconstructions (NRecon version 1.6.4.1) and bone histomorphometric

analyses in two and three dimensions (CT-Analyzer, version 1.13.5.1+) (31). The trabecular bone analysis in tibiae was made in the proximal metaphysis. A reference point was chosen that corresponds to the appearance of secondary spongiosa, and 50 tomograms below this reference point were left unanalyzed before the analysis was made on 250 tomograms. The cortical bone was excluded by operator-drawn regions of interest, and three-dimensional algorithms were used to determine the relevant parameters including bone volume fraction [expressed as percentage of bone volume (BV) over tissue volume (TV), trabecular thickness (Tb.Th), trabecular number (Tb.N), trabecular separation (Tb.Sp), structure model index (SMI), trabecular bone pattern factor (TBPf), and the degree of anisotropy (DA)]. Analysis of cortical bone was performed along a 0.49-mm-long segment (or 100 tomograms) at 37% and 50% of the full length of the tibia calculated from its proximal end. For analysis of the cortical bone compartment, two-dimensional computation was used, and parameters were determined for each of the 100 tomograms and then averaged. Parameters included the following: total cross-sectional area (Tt.Ar), cortical bone area (Ct.Ar), cortical bone perimeter (Ct.Pm), cross-sectional thickness (Ct.Th), and medullary area (Ma.Ar). Cortical and trabecular bone architecture was also evaluated in L4 and L5 vertebrae using the same settings as for tibiae. The region of interest included the whole body of vertebrae.

BMD measurement in vertebrae

BMD analysis in lumbar vertebrae (L4 and L5) was performed with Skyscan software (CT-Analyzer, version 1.13.5.1+). BMD is defined as the volumetric density of calcium hydroxyapatite in grams per cubic centimeter. Two Skyscan-supplied bone phantoms with known BMD values of 0.25 and 0.75 g/cm3 calcium hydroxyapatite were scanned and reconstructed with the same methods and parameters as the vertebrae.

Mechanical testing of femora

Femora were excised immediately after the animals were killed, individually stored in saline soaked gauze, and frozen at −20°C. Immediately before testing, they were thawed and immersed in saline solution during the whole analysis. Three-point bending test of femora from NT and bGH mice was performed as previously described (32). This test allows the calculation of a number of bone mechanical properties, including resistance to bending under load (stiffness), the maximum load that a bone can sustain prior to breaking (maximum load), and the amount of energy the bone can absorb before failure (toughness). Calculations of bone mechanical properties included Young's modulus, a measure of the resistance of a material to elastic deformation under load, and ultimate stress, which is the maximum load normalized by the geometry of the bone midshaft.

Bone histomorphometry

Tibia were fixed in 10% neutral-buffered formalin for 24 hours, dehydrated, and embedded in methyl metacrylate at low temperature to preserve enzymatic activity (33). Unstained 8-µm-thick sections were used for fluorescence microscopy to assess mineral apposition rate (MAR; micrometers per day). Mineralizing surfaces were expressed as alizarin red-labeled surfaces per bone surfaces (MS/BS; percentage), and the bone formation rate was calculated as MS/BS × MAR [bone formation rate per bone surface (BFR/BS); cubic micrometers per square micrometer per day)] (34). Alternatively, sections were stained for tartrate-resistant acid phosphatase (TRAP) (Leucognost SP; Merck) and counterstained with Weigert hematoxylin solution. Histomorphometric parameters were measured on the trabecular bone of the metaphysis on a region of interest consisting of 2 mm width below the growth plate after Goldner's trichrome staining of sections. Measurements were performed using image analysis software (Tablet' measure; Explora Nova). Histomorphometric parameters were reported in accordance with the American Society for Bone and Mineral Research Committee nomenclature (35). L4 vertebrae preserved at 4° after micro-CT analysis were processed in methyl metacrylate as described above and used to assess mineral and apposition rates. TRAP staining was not possible in those vertebrae due to the loss of enzymatic activity.

PTH measurement

Serum PTH levels were measured using a commercial mouse PTH 1–84 ELISA kit (Immutopics).

Statistical analysis

The results were presented as mean ± SD. Comparisons between groups for all data were performed using an unpaired t test (two tailed). Differences were considered significant at $P < .05$. All statistical analyses were performed using GraphPad Prism Software (GraphPad Software Inc). Linear regression analysis with adjustment for body weight was performed using SPSS.

Results

bGH mice have increased body weight and bone length compared with their littermate controls

Five-month-old hemizygous male bGH mice were compared with age- and sex-matched NT controls (n = 16/group). As expected, bGH transgenic mice displayed significant increases in body weight (Figure 1A). Bone lengths of tibia, femora, and lumbar vertebra (total length of L4 and L5) were measured using micro-CT. All bones were consistently longer in bGH mice compared with NT mice (Figure 1, B–D).

bGH mice have lower trabecular bone volume fraction in the tibial metaphysis compared with their littermate controls

Using micro-CT imaging, we found that the trabecular bone volume fraction (BV/TV) was significantly reduced in the bGH mice compared with the NT mice, indicating that bGH mice have low bone mass. This was the case when results were expressed both as direct measurements or when they were adjusted for bone length differences between NT and bGH mice (Table 1). The bone structural analysis showed that the lower BV/TV was due to a reduction in both trabecular thickness and number, although the reduction in trabecular thickness was more highly significant (Table 1). The significant decrease in BV/TV in bGH mice was confirmed by histomorphometry measurements (Table 2). The significant increases in trabecular pattern factor and SMI in bGH mice indicate less intertrabecular connectivity, suggesting deterioration of trabecular bone microarchitecture in those mice (Table 1). The degree of anisotropy was significantly decreased in bGH mice compared with NT mice (Table 1), indicating increased isotropic structure in bGH mice.

bGH mice have increased bone perimeter but lower cortical bone thickness in tibiae compared with their littermate controls

Cortical bone architecture was also analyzed at 37% and 50% of tibia length from its proximal end. Similar data were obtained at both lengths, and Table 1 illustrates the results at 37% of tibia length. Although cortical bone area was similar in bGH and NT mice, total cross-sectional area, cortical bone perimeter, and medullary area were increased and cross-sectional thickness significantly decreased in bGH mice compared with NT mice (Table 1), suggesting that bone size and geometry are different in bGH mice. All these differences remained highly significant after correction for tibiae length. In contrast, only the decrease in cortical thickness in bGH mice remained significant after adjustment for body weight.

bGH mice have decreased bone cortical mineral density and changes in trabecular and cortical structural parameters in vertebrae compared with their littermate controls

BMD was evaluated in fourth and fifth lumbar vertebrae (L4 and L5). Similar results were obtained for both vertebrae, and we have illustrated the results obtained on the fifth lumbar vertebrae. We did not measure significant differences in the BMD of the trabecular compartment in the vertebrae between bGH and NT mice (Figure 2A), whereas the BMD in the cortical compartment was significantly decreased in bGH vertebrae compared with NT ones (Figure 2B). BV/TV was not different in bGH and NT mice vertebrae, except when adjusted for bone length (Table 3). Trabecular thickness was significantly decreased in bGH vertebrae compared with the NT group, even after

adjustment for length and body weight, although histomorphometry data showed only a trend for a decrease (Tables 3 and and4).4). Other trabecular parameters were not consistently affected. Significant differences were also observed in cortical bone because L4 and L5 vertebrae in bGH group showed increased bone cortical area but decreased cortical thickness (Table 3). However, only cortical thickness remained significant after correction for both body weight and vertebrae length.

bGH mice have decreased mechanical strength in tibiae compared with their littermate controls

To investigate bone mechanical properties of bGH mice, their femurs were removed at 5 months and subjected to three-point bending tests. Data on the mechanical strength of the femurs are shown in Figure 3. Compared with the NT group, bGH had weaker bones, as illustrated by significantly reduced ultimate stress (Figure 3A) and Young's modulus (Figure 3B). There was also a trend for a reduced stiffness in bGH mice compared with NT mice, close to significance (Figure 3C).

bGH mice have increased bone remodeling compared with their littermate controls

To determine the cause of the low trabecular bone mass in bGH mice, we examined bone cellular activities in the tibia of those mice, using bone histomorphometry. Histomorphometric assessment confirmed our micro-CT findings that trabecular BV/TV in tibial metaphysis is significantly decreased in bGH compared with NT mice (Figure 4A and Table 2). Analysis of mineralizing apposition and bone formation rates using double-fluorescence labeling showed that bGH mice have a higher bone formation rate than NT mice (Figure 4C). MAR was significantly increased (Table 2). The percentage of TRAP-positive surfaces (representing resorption surfaces) was also significantly higher in the bGH mice compared with NT mice (Figure 4B). These results indicate that the bGH mice have a higher trabecular bone turnover compared with their littermates controls, which is associated with a low trabecular bone mass phenotype. The increased bone formation rate in bGH mice compared with their littermate controls was also observed in vertebrae (Table 4). We also measured serum PTH levels in our mice, and we found significantly increased PTH levels in 5-month-old male bGH mice compared with littermate controls (Figure 4D).

Discussion

This study shows that bGH mice with elevated serum GH levels have compromised bone architecture, characteristic that often mimics the skeletal changes experienced by acromegaly patients. The use of bGH mice is a valuable model for the study of skeletal changes in response to excess GH that occur in acromegaly patients. The advantage of this experimental mouse model is that there is no associated hypogonadism (36), so it is easier to decipher the skeletal effects of

excess GH than in acromegaly patients. There is, however, a major difference between the bGH mouse model and acromegaly patients as in patients' overexpression of GH usually occurs after epiphyseal closure. Conversely, overexpression of GH in bGH mice occurs in utero and through adult life. Thus, it is possible that the temporal control of GH overexpression has implications on bone regulation.

Our works shows that bGH mice have significant increases in total body weight and in bone lengths. This supports previous studies that demonstrated that human GH and bGH transgenic mice are larger and exhibit disproportionate skeletal gigantism (28,–30, 37, 38). Bone sizes are increased in bGH mice (30), and treatment of growing rats with human GH rats leads to an increase in bone size (39). Elevated levels of GH appear to be the main cause for gigantism in those mice rather than an increase in mechanical loading as a result of increased body weight (40).

Bone architecture in bGH mice has been poorly studied. GH has complex effects on bone that vary, depending on the skeletal compartments and different sites. Using high-resolution micro-CT, we found that bGH mice have altered cortical and trabecular bone architecture in long bones. Analysis of trabecular bone in tibia shows that despite an increase in bone length, bGH mice have significantly lower bone volume fraction (BV/TV) and trabecular number and thickness than littermate controls, indicating a low trabecular bone mass in those mice. In addition, measurements of parameters reflecting the structure and the geometry of trabecular bone clearly demonstrate less intertrabecular connectivity and more rod-like structures in trabecular bone of bGH mice, representing a deterioration of trabecular bone quality that is similar to what is observed with aging and in osteoporosis (41) and in agreement with most clinical studies (20). Cortical bone thickness was also significantly decreased in tibia despite increases in total cross-sectional area, cortical tissue perimeter, and medullary area, reflecting the bigger tibia in bGH mice. Previous micro-CT analysis of GH transgenic mice did not show any major change in trabecular bone volume fraction in male mice. In contrast, female transgenic mice showed an increase in trabecular bone fraction volume in femora (29). This discrepancy could be due to a different mouse genetic background and/or the age of the mice because the transgenic mice used in our study are older (5 mo vs 3 mo in the previous study). Our resolution for micro-CT analysis of bone architecture was also 10 times higher than that used in the former study (29).

Because there is an increased prevalence of vertebral fractures in acromegaly patients (12), we also examined bone architecture and BMD in vertebrae of bGH mice. Surprisingly, there were no significant changes in trabecular BMD and bone volume fraction in L4 and L5 vertebrae of bGH mice compared with controls but a decrease in trabecular thickness. Cortical bone was more significantly

affected because bGH mice have significantly lower cortical BMD and cortical thickness in the lumbar vertebrae than their controls. Although cortical bone density was also previously shown to be significantly lower in femora of bGH transgenic mice (30), these results in mouse models conflict with clinical records whereby elevated GH levels are often linked to increased cortical BMD in humans (1, 19, 20, 42). Clinical data are, however, mostly based on BMD measurements by dual-energy X-ray absorptiometry, which cannot discriminate between cortical and trabecular compartments, in contrast to micro-CT or peripheral quantitative computed tomography (pQCT). The view of increased cortical BMD in patients with active acromegaly is supported by the fact that these patients have an increase in BMD at the forearm and/or femoral neck, two sites at which cortical bone is the main determinant of bone strength, whereas BMD is less affected at the lumbar spine, a site at which trabecular bone is dominant (19, 43, 44). This was corroborated in a clinical study using high-resolution pQCT, which showed higher cortical density in the distal tibia in patients with active acromegaly compared with controlled acromegaly (20), suggesting that high resolution pQCT should allow better in vivo assessments of the bone architecture in acromegaly patients in the future.

Interestingly, studies conducted in childhood- and adult-onset GHD have also shown reduced cortical bone (45) and GH therapy in GHD patients seems to have a greater effect on cortical than on trabecular bone (46). Our data support previous conclusions demonstrating that the skeletal effects of GH depend on the compartment and the site analyzed, and this may be due to changes in vascular supply, response to sex steroids, and/or mechanical loading (19). We used only males in our study to restrict the differences in cortical density between sexes. We analyzed bone architecture at two sites with a very different ratio in cortical and trabecular bone but that are also subject to different loading environments. We therefore cannot exclude that the differences in bone architecture between bGH mice tibiae and vertebrae depend on mechanical sensitivity to loading, which is essential for the maintenance of the skeleton in both humans and animals. Previous studies have shown that the GH/IGF-1 signaling pathway is regulated by in vivo mechanical loading (47).

At all sites examined, our data suggest a deterioration of bone architecture. This was confirmed by the decreased intrinsic material properties of femora of bGH mice, leading to a reduction in bone strength, which may explain the higher rate of fractures in acromegaly patients. Decreased trabecular bone biomechanical competence was also observed in acromegaly patients (48). Interestingly, it was shown that local production of human GH in osteoblasts in a model of transgenic mice induces bone growth as expected but impaired the bones mechanical properties (49). In contrast, erythroid-specific expression of human GH leads to bones with high bone density and increased biomechanical properties (50). This suggests that localized GH expression could have

opposing effect to global GH expression as observed in our study. In models of GHD, bone mechanical properties are also not always rescued with GH treatment (51). It is, however, puzzling that acromegalic patients have a higher prevalence of vertebral fractures because our data suggest that trabecular architecture in bGH vertebrae is less deteriorated than in tibiae.

The cortex also contributes to a significant part of vertebral bone strength (52) and other bone quality parameters, such as collagen content, and morphology may play a role. It is also important to point out that the spine in the mouse is not a good model of the spine in humans because it has almost no load bearing. Bone strength depends on bone morphology and composition that can be associated with changes in bone turnover rate. Our results indicate that bone turnover is largely increased in the trabecular bone of adult bGH mice tibia. We also found an increase in the number of mineralizing surfaces and osteoclasts on bone surfaces, suggesting that bone cell numbers and activities are both stimulated in bGH mice compared with controls. To our knowledge, this is the first demonstration of accelerated bone turnover in favor of bone resorption in the skeleton of bGH mice, and this may explain the deterioration of bone mechanical strength in these mice. Bone turnover markers in acromegaly patients are also increased (19) and GH treatment is effective in enhancing bone turnover (46, 53, 54). The increased bone turnover in bGH mice suggests that the deterioration of bone architecture observed in those mice is not the consequence of changes occurring during bone development that can affect bone architecture later in life. The increase in cortical perimeter together with the decrease in cortical thickness observed in bGH mice suggest that endosteal bone resorption and periosteal bone formation are both enhanced, which explains the increase in bone size. Interestingly, we found a similar increased bone formation rate in the vertebral trabecular bone of bGH mice compared with controls, suggesting that bone cellular activities are also stimulated in vertebrae, although this needs to be confirmed in case of osteoclast activity.

The mechanisms leading to the enhanced bone turnover in bGH mice whose net balance is bone resorption is yet unclear. Our data show increased PTH levels in bGH mice, which could contribute to this greater bone turnover (55). GH transgenic mice have also hyperinsulinemia despite euglycemia (56). Other possible mechanisms include stimulation by GH and IGF-1 of proinflammatory cytokines that may promote osteoclastogenesis (57). A very exciting future aspect of this work will be to determine which direct or indirect signaling pathways link the excess GH in our mouse model to these deleterious effects on bone. GHR affects many signaling pathways, the major one being the JAK/STAT but additional independent pathways have been identified (58). Among the pathways affected by GHR activation and JAK2 are the MAPK and phosphatidylinositol 3-kinase/Akt pathways, which play crucial roles in the differentiation, function, and survival of bone

cells (59). GH also regulates IGF-1 expression that has direct effects on bone via IGF-1 receptor and downstream signaling cascades critical for bone cell survival and metabolism (60). It is also possible that in our mouse model, the high GH tone may lead to feedback inhibition. Recent studies have indicated that GHR activation induces suppression of cytokine signaling (SOCS) proteins, which in turn inhibit GH signaling through a negative feedback mechanism. SOCS play important roles in skeletal development and osteoclastogenesis (61).

In conclusion, our data collectively indicate that elevated serum GH levels have negative effects on bone architecture and quality in male mice. Combining, for the first time, high-resolution micro-CT measurements of skeletal architecture in trabecular and cortical compartments, bone mechanical testing, and quantification of bone cellular activities, we show that bGH mice display characteristics of the skeletal changes observed in acromegaly patients, which vary according to the skeletal site. Our study is limited by the fact that we have only analyzed males and only at one particular time point; therefore, we cannot exclude that bGH female mice may behave differently because the skeletal effects of GH may be influenced by sex steroids and mechanical loading. It, however, supports the notion that bone strength is decreased in acromegaly patients and that this may not always be reflected in the measurement of BMD. The inability of BMD to predict fracture risk in acromegaly patients is also true in diabetic patients (62) and clearly demonstrates the need for a better understanding of factors affecting bone quality in patients with altered GH and IGF-1 metabolism.

Acknowledgments

This work was supported by the Society for Endocrinology.

Disclosure Summary: The authors have nothing to disclose

Abbreviations

BFR/BS: bone formation rate per bone surface
bGH: bovine GH
BMD: bone mineral density
BV: bone volume
Ct.Ar: cortical bone area
Ct.Pm: cortical bone perimeter
Ct.Th: cross-sectional thickness
DA: degree of anisotropy
GHD: GH deficiency

GHR: GH receptor
JAK: Janus kinase
Ma.Ar: medullary area
MAR: mineral apposition rate
micro-CT: microcomputed tomography
MS/BS: mineralizing surfaces per bone surface
NT: nontransgenic
pQCT: peripheral quantitative computed tomography
SMI: structure model index
STAT: signal transducer and activator of transcription
Tb.N: trabecular number
Tb.Sp: trabecular separation
Tb.Thtrabecular thickness
TBPf: trabecular bone pattern factor
TRAP: tartrate-resistant acid phosphatase
Tt.Ar: total cross-sectional area
TV: tissue volume

References

1. Ohlsson C, Bengtsson BA, Isaksson OG, Andreassen TT, Slootweg MC. Growth hormone and bone. Endocr Rev. 1998;19:55–79. [PubMed: 9494780]

2. Ohlsson C, Nilsson A, Isaksson OG, Lindahl A. Effect of growth hormone and insulin-like growth factor-I on DNA synthesis and matrix production in rat epiphyseal chondrocytes in monolayer culture. J Endocrinol. 1992;133:291–300.[PubMed: 1613431]

3. Tritos NA, Biller BM. Growth hormone and bone. Curr Opin Endocrinol Diabetes Obes. 2009;16:415–422.[PubMed: 19770650]

4. Vijayakumar A, Novosyadlyy R, Wu Y, Yakar S, LeRoith D. Biological effects of growth hormone on carbohydrate and lipid metabolism. Growth Horm IGF Res. 2010;20:1–7. [PMCID: PMC2815161] [PubMed: 19800274]

5. Gent J, van Kerkhof P, Roza M, Bu G, Strous GJ. Ligand-independent growth hormone receptor dimerization occurs in the endoplasmic reticulum and is required for ubiquitin system-dependent endocytosis. Proc Natl Acad Sci USA. 2002;99:9858–9863. [PMCID: PMC125043] [PubMed: 12105275]

6. Giustina A, Mazziotti G, Canalis E. Growth hormone, insulin-like growth factors and the skeleton. Endocr Rev. 2008;29:535–559. [PMCID: PMC2726838] [PubMed: 18436706]

7. Courtland H-W, Sun H, Beth-On M, et al. Growth hormone mediates pubertal skeletal development independent of hepatic IGF-1 Production. J Bone Miner Res. 2011;26:761–768. [PMCID: PMC3179330] [PubMed: 20928887]

8. Melmed S. Acromegaly pathogenesis and treatment. J Clin Invest. 2009;119:3189–3202. [PMCID: PMC2769196][PubMed: 19884662]

9. Thomas JD, Monson JP. Adult GH deficiency throughout lifetime. Eur J Endocrinol. 2009;161:S97–S106.[PubMed: 19684058]

10. Colao A, Di Somma C, Pivonello R, et al. Bone loss is correlated to the severity of growth hormone deficiency in adult patients with hypopituitarism. J Clin Endocrinol Metab. 1999;84:1919–1924. [PubMed: 10372687]

11. Claessen KM, Kroon HM, Pereira AM, et al. Progression of vertebral fractures despite long-term biochemical control of acromegaly: a prospective follow-up study. J Clin Endocrinol Metab. 2013;98:4808–4815. [PubMed: 24081732]

12. Padova G, Borzi G, Incorvaia L, et al. Prevalence of osteoporosis and vertebral fractures in acromegalic patient. Clin Cases Miner Bone Metab. 2011;8:37–43. [PMCID: PMC3279059] [PubMed: 22461828]

13. Mazziotti G, Bianchi A, Bonadonna S, et al. Prevalence of vertebral fractures in men with active acromegaly. J Clin Endocr Metab. 2008;93:4649–4655. [PubMed: 18827004]

14. Wassenaar MJ, Biermasz NR, Hamdy NA, et al. High prevalence of vertebral fractures despite normal bone mineral density in patients with long-term controlled acromegaly. Eur J Endocrinol. 2011;164:475–483. [PubMed: 21257726]

15. Mazziotti G, Bianchi A, Porcelli T, et al. Vertebral fractures in patients with acromegaly: a 3-year prospective study. J Clin Endocrinol Metab. 2013;98:3402–3410. [PubMed: 23771918]

16. Mormando M, Nasto LA, Bianchi A, et al. Growth hormone receptor isoforms and skeletal fragility in acromegaly. Eur J Endocrinol. 2014;171:237–245. [PubMed: 24866575]

17. Jean Ho P, Lorraine M, Barkan A, Shaporo B. Bone mineral density of the axial skeleton in acromegaly. J Nucl Med. 1992;33:1608–1612. [PubMed: 1517833]

18. Kayath Mj, Viera JG. Osteopenia occurs in a minority of patients with acromegaly and is predominant in the spine. Osteoporosis Int. 1997;7:226–230.

19. Bolanowski M, Daroszewski J, Medras M, Zadrozna-Sliwka B. Bone mineral density and turnover in patients with acromegaly in relation to sex, disease activity and gonadal function. J Bone Miner Metab. 2006;24:72–78.[PubMed: 16369902]

20. Madeira M, Neto LV, de Paula Paranhos Neto F, et al. Acromegaly has a negative influence on trabecular bone, but not on cortical bone, as assessed by high resolution peripheral quantitative computed tomography. J Clin Endocrinol Metab. 2013;98:1734–1741. [PubMed: 23482608]

21. Vestergaard P, Mosekilde L. Fracture risk is decreased in acromegaly: a potential beneficial effect of growth hormone. Osteoporosis Int. 2004;15:155–159.

22. Felsenberg D, Boonen S. The bone quality framework: determinants of bone strength and their interrelationships, and implications for osteoporosis management. Clin Ther. 2005;27:1–11. [PubMed: 15763602]

23. Borah B, Gross GJ, Dufresne TE, et al. Three dimensional microimaging (MRmicroI and microCT), finite element modeling, and rapid prototyping provide unique insights into bone architecture in osteoporosis. Anat Rec. 2001;265:101–110. [PubMed: 11323772]

24. Chavassieux P, Seeman E, Delmas PD. Insights into material and structural basis of bone fragility from diseases associated with fractures: how determinants of the biomechanical properties of bone are compromised by disease. Endocr Rev. 2007;28:151–164. [PubMed: 17200084]

25. Kopchick JJ, Bellush LL, Coschigano KT. Transgenic models of growth hormone action. Annu Rev Nutr. 1999;19:437–461. [PubMed: 10448532]

26. Turner ND, Knapp JR, Byers FM, Kopchick JJ. Physical and mechanical characteristics of tibias from transgenic mice expressing mutant bovine growth hormone genes. Exp Biol Med. 2001;226:133–139.

27. Berryman DE, List EO, Coschigano KT, Behar K, Kim JK, Kopchick JJ. Comparing adiposity profiles in three mouse models with altered GH signaling. Growth Horm IGF Res. 2004;14:309–318. [PubMed: 15231300]

28. Wolf E, Rapp K, Brem G. Expression of metallothionein-human growth hormone fusion genes in transgenic mice results in disproportionate skeletal gigantism. Growth Dev Aging. 1991;55:117–127. [PubMed: 1938045]

29. Eckstein F, Lochmüller EM, Koller B, et al. Body composition, bone mass and microarchitectural analysis in GH-transgenic mice reveals that skeletal changes are specific to bone compartment and gender. Growth Horm IGF Res. 2002;12:116–125. [PubMed: 12175649]

30. Eckstein F, Weusten A, Schmidt C, et al. Longitudinal in vivo effects of growth hormone overexpression on bone in transgenic mice. J Bone Miner Res. 2004;19:802–810. [PubMed: 15068504]

31. Shah M, Kola B, Bataveljic A, et al. AMP-activated protein kinase (AMPK) activation regulates in vitro bone formation and bone mass. Bone. 2010;147:309–319. [PMCID: PMC3629687] [PubMed: 20399918]

32. Marenzana M, Greenslade K, Eddleston A, et al. Sclerostin antibody treatment enhances bone strength but does not prevent growth retardation in young mice treated with dexamethasone. Arthritis Rheum. 2011;63:2385–2395.[PubMed: 21484764]

33. Chappard D, Palle S, Alexandre C, Vico L, Riffat G. Bone embedding in pure methyl methacrylate at low temperature preserves enzyme activities. Acta Histochem. 1987;81:183–190. [PubMed: 3111154]

34. Chavassieux P, Arlot M, Meunier PJ. Clinical use of bone biopsy. In: Marcus R, Feldman D, Kelsey J, editors. , eds. Osteoporosis. 2nd ed San Diego: Academic Press; 2001:501–509.

35. Dempster DW, Compston JE, Drezner MK, et al. Standardized nomenclature, symbols and units for bone histomorphometry. A 2012 update of the report of the ASBMR histomorphometry nomenclature committee. J Bone Miner Res. 2013;28:1–16. [PMCID: PMC3672237] [PubMed: 23197339]

36. Cecim M, Kerr J, Bartke A. Effects of bovine growth hormone (bGH) transgene expression or bGH treatment on reproductive functions in female mice. Biol Reprod. 1995;52:1144–1148. [PubMed: 7626714]

484 37. Wanke R, Wolf E, Hermanns W, Folger S, Buchmüller T, Brem G. The GH-transgenic
485 mouse as an experimental model for growth research: clinical and pathological
486 studies. Horm Res. 1992;37:74–87. [PubMed: 1427647]

487 38. Wolf E, Rapp K, Wanke R, et al. Growth characteristics of metallothionein-human growth
488 hormone transgenic mice as compared to mice selected for high eight-week body weight
489 and unselected controls. II. Skeleton Growth Dev Aging. 1991;55:237–248.

490 39. Rosen HN, Chen V, Citadini A, et al. Treatment with growth hormone and IGF-1 in
491 growing rats increases bone mineral content but not bone mineral density. J Bone Miner
492 Res. 1995;10:1352–1358. [PubMed: 7502707]

493 40. Palmer AJ, Chung M-Y, List EO, et al. Age-related changes in body composition of bovine
494 growth hormone transgenic mice. Endocrinology. 2009;150:1353–1360. [PMCID:
495 PMC2654748] [PubMed: 18948397]

496 41. Borah B, Dufresne TE, Chmielewski PA, Johnson TD, Chines A, Manhart MD. Risedronate
497 preserves bone architecture in postmenopausal women with osteoporosis as measured by
498 three-dimensional microcomputed tomography. Bone. 2004;34:736–746. [PubMed:
499 15050906]

500 42. Kaji H, Sugimoto T, Nakaoka D, Okimura Y, Abe H, Chihara K. Bone metabolism and body
501 composition in Japanese patients with active acromegaly. Clin Endocrinol (Oxf).
502 2001;55:175–181. [PubMed: 11531923]

503 43. Biermasz N, Hamdy NAT, Pereira AM, Romijn JA, Roelsema F. Long-term maintenance of
504 the anabolic effects of GH on the skeleton in successfully treated patients with
505 acromegaly. Eur J Endocrinol. 2005;152:53–60. [PubMed: 15762187]

506 44. Chiodini I, Trischitta V, Carnevale V, Liuzzi A, Scillitani A. Bone mineral density in
507 acromegaly: does growth hormone excess protect against osteoporosis? J Endocrinol Invest.
508 2001;24:288–291. [PubMed: 11383916]

509 45. Murray RD, Adams JE, Shalet SM. A densitometric and morphometric analysis of the
510 skeleton in adults with varying degrees of growth hormone deficiency. J Clin Endocrinol
511 Metab. 2006;91:432–438. [PubMed: 16278268]

512 46. Bravenboer N, Holzmann PJ, Ter Maaten PJ, Stururman LM, Roos JC, Lips P. Effect of
513 long-term growth hormone treatment on bone mass and bone metabolism in growth
514 hormone-deficient men. J Bone Miner Res. 2005;20:1778–1784.[PubMed: 16160735]

515 47. Rejnders CM, Bravenboer N, Holzmann PJ, Bhoelan F, Blankenstein MA, Lips P. In vivo
516 mechanical loading modulates insulin-like growth factor binding protein-2 gene expression
517 in rat osteocytes. Calcif Tissue Int. 2007;80:137–143. [PMCID: PMC1914289] [PubMed:
518 17308996]

519 48. Ueland T, Ebbesen EN, Thomsen JS, et al. Decreased trabecular bone biomechanical
520 competence, apparent density, IGF-II and IGHBP-5 content in acromegaly. Eur J Clin Invest.
521 2002;32:122–128. [PubMed: 11895459]

522 49. Tseng KF, Bonadio JF, Stewart TA, Baker AR, Goldstein SA. Local expression of human
523 growth hormone in bone results in impaired mechanical integrity in the skeletal tissue of
524 transgenic mice. J Orthop Res. 1996;14:598–604.[PubMed: 8764869]

525 50. Steinke B, Patwardhan AG, Havey RM, King D. Human growth hormone transgene
526 expression increases the biomechanical structural properties of mouse vertebrae. Spine.
527 1999;24:1–4. [PubMed: 9921583]

528 51. Kristensen E, Hallfrimsson B, Morck DW, Boyd SK. Microarchitecture, but not bone
529 mechanical properties, is rescued with growth hormone treatment in a mouse model of
530 growth hormone deficiency. Int J Endocrinol. 2012;2012:294965. [PMCID:
531 PMC3312192] [PubMed: 22505889]

532 52. Roux JP, Wegrzyn J, Arlot ME, et al. Contribution of trabecular and cortical
533 compartments to biomechanical behaviour of human vertebrae: an ex vivo study. J Bone
534 Miner Res. 2010;25:356–361. [PubMed: 19653808]

535 53. Gotherstrom G, Svensson J, Koranyi J, et al. A prospective study of 5 years of GH
536 replacement therapy in GH-deficient adults: sustained effects on body composition, bone
537 mass and metabolic indices. J Clin Endocrinol Metab. 2001;86:4657–4665. [PubMed:
538 11600522]

539 54. Bredella MA, Gerweck AV, Barber LA, et al. Effects of growth hormone administration for
540 6 months on bone turnover and bone marrow fat in obese premenopausal women. Bone.
541 2014;62:29–35. [PMCID: PMC4014200][PubMed: 24508386]

542 55. Kamenicky P, Blanchard A, Gauci C, et al. Pathophysiology of renal calcium handling in
543 acromegaly: what lies behind hypercalciura? J Clin Endocrinol Metab. 2012;97:2124–
544 2133. [PubMed: 22496496]

545 56. Kopchick JJ, List EO, Kelder B, Gosney ES, Berryman DE. Evaluation of growth hormone
546 (GH) action in mice: discovery of GH receptor antagonists and clinical indications. Mol Cell
547 Endocrinol. 2014;386:34–45. [PMCID: PMC3943600] [PubMed: 24035867]

548 57. Locatelli V, Bianchi VE. Effect of GH/IGF-1 on bone metabolism and osteoporosis. Int J
549 Endocrinol. 2014;2014:235060. [PMCID: PMC4132406] [PubMed: 25147565]

550 58. Brooks AJ, Wei Wooh J, Tunny KA, Waters MJ. Growth hormone receptor; mechanism of
551 action. Int J Biochem Cell Biol. 2008;40:1984–1989. [PubMed: 17888716]

552 59. Marie PJ. Signaling pathways affecting skeletal health. Cur. Osteoporosis Rep.
553 2012;10(3):190–198.

554 60. Guntur AR, Rosen CJ. IGF-1 regulation of key signalling pathways in bone. Bonekey Rep.
555 2013;2:437. [PMCID: PMC3818534] [PubMed: 24422135]

556 61. Ahmed SF, Farquharson C. The effect of GH and IGF1 in linear grow and skeletal
557 development and their modulation by SOCS proteins. J Endocrinol. 2010;206:249–
558 259. [PubMed: 20631046]

559 62. Yamamoto M, Yamaguchi T, Yamauchi M, Kaji H, Sugimoto T. Diabetic patients have an
560 increased risk of vertebral fractures independent of BMD and diabetic complications. J Bone
561 Miner Res. 2009;24:702–709. [PubMed: 19049338]

Figures and Tables

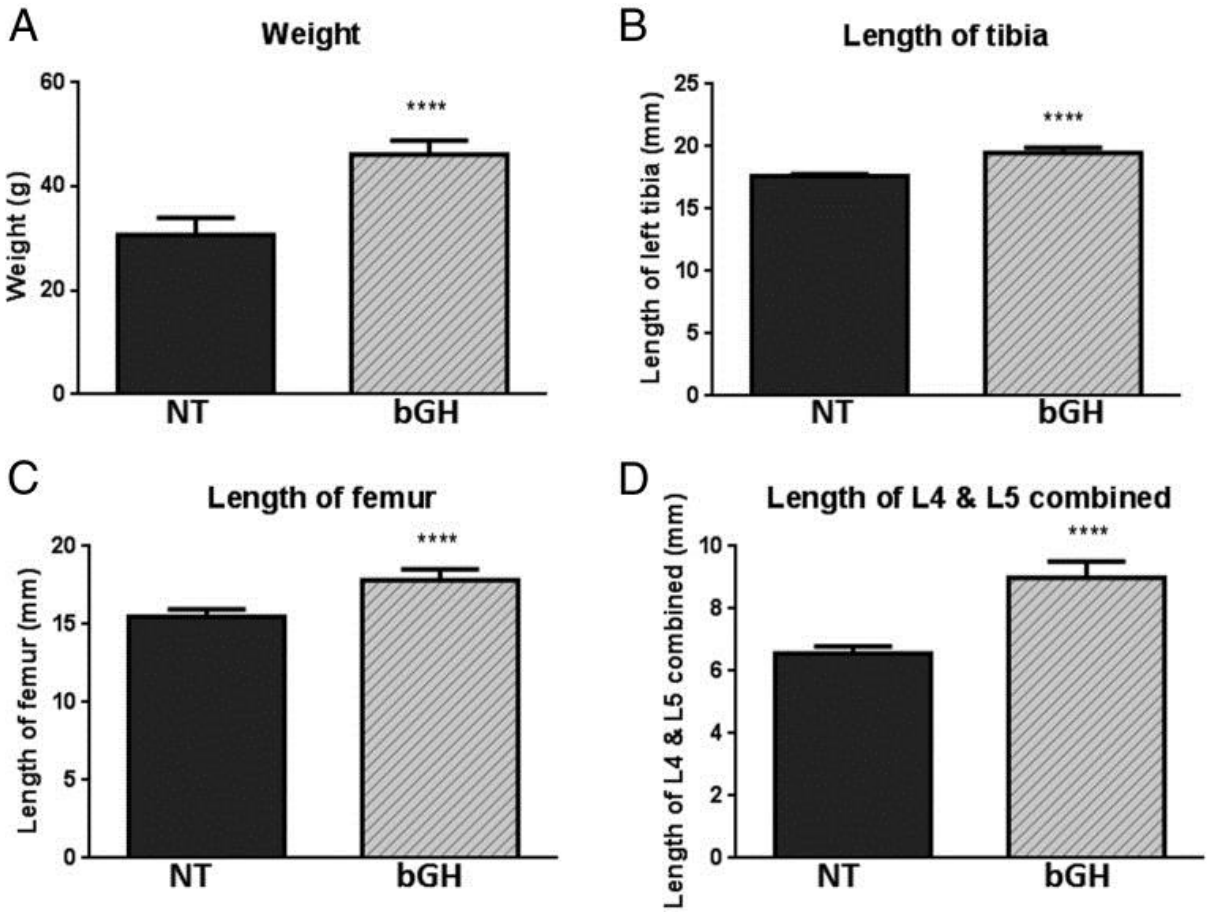

Figure 1: bGH mice have increased body weights and bone lengths.

NT and bGH mice were weighed at 5 months of age and lengths of tibiae, femora, and lumbar vertebrae measured using micro-CT. Body weights (A) and lengths of tibiae (B), femora (C), and vertebrae (combined L4 and L5) (D) of bGH and NT mice are shown. Values are mean ± SD of n = 16 mice/group. ****, P < .0001 NT vs bGH mice.

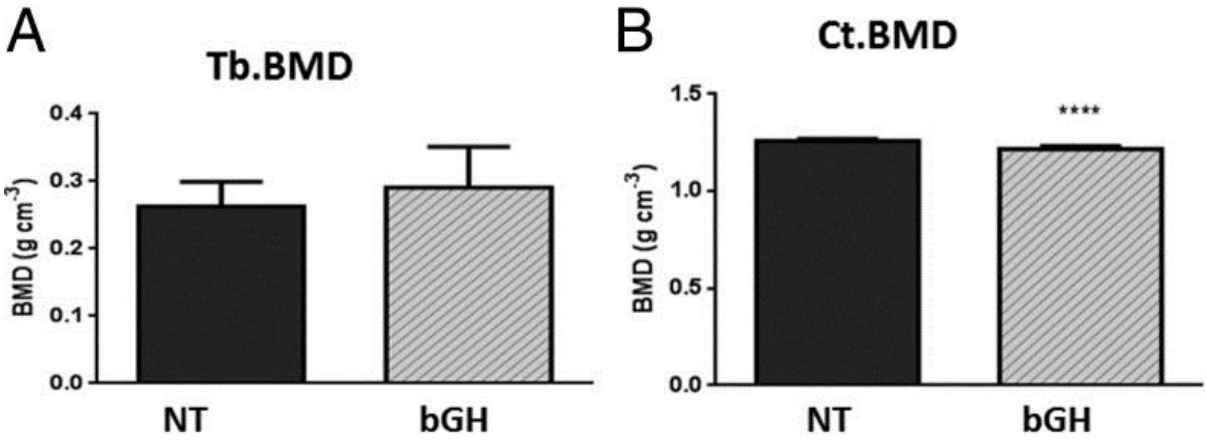

572
573
574 **Figure 2: bGH mice have decreased cortical BMD but not trabecular BMD in vertebrae.**
575
576 Cortical and trabecular BMD were assessed by micro-CT in lumbar vertebrae L5 vertebral body from
577 NT and bGH mice aged 5 months. L5 vertebra vertebral body trabecular BMD (A) and L5 vertebra
578 vertebral body cortical BMD (B) in bGH and NT mice. Bars represent mean ± SD of nine mice per
579 group. ****, P < .0001 NT vs bGH mice. Tb.BMD, trabecular BMD; Ct.BMD, cortical BMD.
580
581
582
583
584
585
586

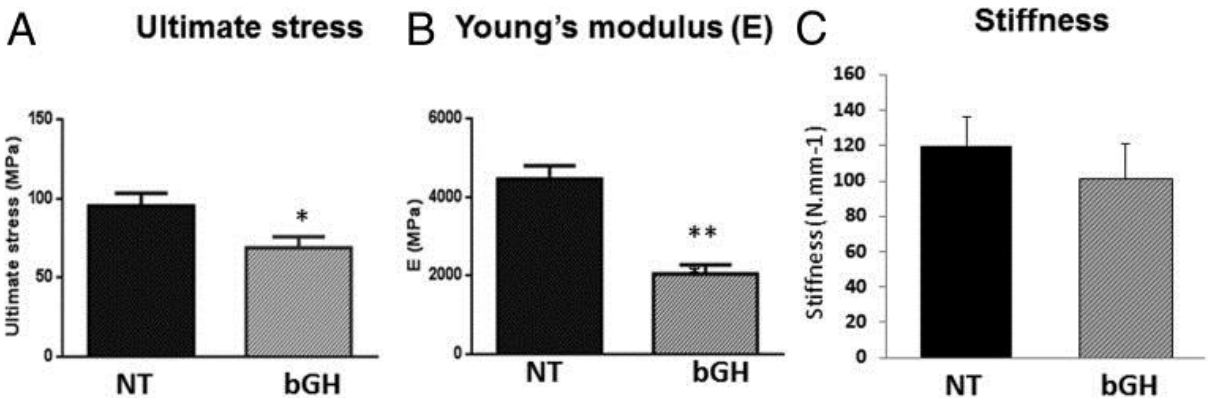

587
588
589 **Figure 3: Mechanical testing (three point bending) of femora from bGH and NT mice.**
590 Biomechanical properties of the excised mouse femurs in NT and bGH mice aged 5 months using the
591 three-point bending test, which tested for ultimate stress (A), Young's modulus (B), and stiffness (C).
592 Bars represent mean ± SD of six mice per group. *, P < .05, **, P < .001 NT vs bGH mice.
593
594
595
596
597

598 **Table 1:** Trabecular and Cortical Bone Parameters in Tibiae of NT and bGH Mice Aged 5 Months

	NT Mice	bGH Mice	Results Expressed as a Ratio of Tibia Length (×100)	
			NT Mice	bGH Mice
BV/TV, %	5.430 ± 0.647	3.061 ± 0.408[a]	30.802 ± 10.304	15.685 ± 6.667[b]
Tb.N, 1/mm	1.640 ± 0.245	1.114 ± 0.155[c]	9.304 ± 3.980	5.706 ± 2.382[c]
Tb.Th, mm	0.035 ± 0.002	0.028 ± 0.001[b]	0.201 ± 0.035	0.144 ± 0.015[b]
Tb.Sp, mm	0.373 ± 0.038	0.391 ± 0.039	2.115 ± 0.815	2.016 ± 0.760
TBPf, 1/mm	8.873 ± 4.373	31.13 ± 3.835[b]	50.220 ± 70.117	160.118 ± 66.80[b]
SMI	1.208 ± 0.133	1.785 ± 0.105[a]	6.844 ± 2.521	9.189 ± 1.815[a]
DA	2.117 ± 0.062	1.793 ± 0.063[a]	12.006 ± 1.103	9.211 ± 1.034[d]
Tt.Ar, mm^2	1.343 ± 0.036	1.826 ± 0.101[b]	7.608 ± 0.527	9.434 ± 1.149[a] (N)
Ct.Ar, mm^2	0.781 ± 0.021	0.793 ± 0.031	4.427 ± 0.296	4.107 ± 0.386
Ct.Pm, mm	11.87 ± 0.315	16.15 ± 0.743[d]	67.266 ± 5.165	83.528 ± 8.470[a] (N)
Ct.Th, mm	0.131 ± 0.002	0.098 ± 0.002[d]	0.746 ± 0.023	0.512 ± 0.043[d]
Ma.Ar, mm^2	0.561 ± 0.017	1.032 ± 0.074[d]	3.180 ± 0.241	5.326 ± 0.861[d] (N)

599

600 Abbreviation: N, nonsignificant after adjustment by body weight.

601 Results are mean ± SD 16 mice/group.

602 [a]$P < .01$, vs NT mice.
603 [b]$P < .001$, vs NT mice.
604 [c]$P < .05$, vs NT mice.
605 [d]$P < .0001$ vs NT mice.
606

607

608

609

610

611

612

613

614 **Table 2:** Static and Dynamic Trabecular Bone Parameters in bGH Mice Tibiae Compared With NT
615 Tibiae

Histomorphometry Parameters	NT	bGH
BV/TV, %	14.225 ± ± 1.549	8.490 ± 2.867[a]
Tb.N, 1/mm	3.440 ± 0.582	2.380 ± 0.673
Tb.Th, mm	0.042 ± 0.009	0.035 ± 0.003
Tb.Sp, mm	0.255 ± 0.042	0.412 ± 0.150[a]
MS/BS, %	24.34 ± 6.49	40.54 ± 8.34[a]
MAR, µm/d	1.546 ± 0.413	2.329 ± 0.290[a]
BFR/BS, $\mu m^3/\mu m^2/d$	0.387 ± 0.189	1.001 ± 0.163[a]
Oc.S/BS, µm	6.623 ± 1.038	9.895 ± 0.306[a]
Oc.N/BS, 1/mm	2.19 ± 0.54	2.82 ± 0.46

616

617 Mean ± SD (five and six mice per group).

618 [a]$P < .05$ vs NT.

Table 3: Trabecular and Cortical Bone Parameters in Vertebrae of NT and bGH Mice Aged 5 Months

	NT Mice	bGH Mice	Results Expressed as a Ratio of Vertebrae Length	
			NT mice	bGH Mice
BV/TV, %	5.699 ± 1.120	6.151 ± 1.294	1.718 ± 0.323	1.409 ± 0.286[a]
Tb.N, 1/mm	1.578 ± 0.173	2.077 ± 0.357[b]	0.476 ± 0.049	0.475 ± 0.072
Tb.Th, mm	0.035 ± 0.004	0.029 ± 0.001[b]	0.011 ± 0.001	0.006 ± 0.001[b]
Tb.Sp, mm	0.418 ± 0.026	0.462 ± 0.055[a]	0.126 ± 0.009	0.105 ± 0.010[b]
TBPf, 1/mm	−1.515 ± 4.94	−6.590 ± 6.951	−0.446 ± 1.512	−1.454 ± 1.544
SMI	0.739 ± 0.274	0.697 ± 0.235	0.224 ± 0.087	0.161 ± 0.058
DA	1.898 ± 0.544	1.604 ± 0.233[a]	0.572 ± 0.154	0.368 ± 0.054[b]
Tt.Ar, mm^2	0.428 ± 0.017	0.478 ± 0.177	0.129 ± 0.035	0.109 ± 0039
Cs.Ar, mm^2	0.278 ± 0.027	0.326 ± 0.061[b]	0.084 ± 0.007	0.074 ± 0.010[a] (N)
Cs.Pm, mm	12.23 ± 0.632	17.60 ± 2.576[c]	3.698 ± 0.210	4.017 ± 0.357
Cs.Th, mm	0.045 ± 0.003	0.036 ± 0.003[c]	0.013 ± 0.001	0.008 ± 0.001[c]
Ma.Ar, mm^2	0.149 ± 0.100	1.152 ± 0.090	0.045 ± 0.030	0.034 ± 0.031

Abbreviation: N, nonsignificant after adjustment by body weight.

[a] $P < .05$ vs NT mice.
[b] $P < .01$ vs NT mice.
[c] $P < .0001$ vs NT mice.

Table 4: Static and Dynamic Trabecular Bone Parameters in bGH Mice Vertebrae Compared With NT Vertebrae

Histomorphometry Parameters	NT	bGH
BV/TV, %	16.532 ± 3.291	15.198 ± 2.766
Tb.N, 1/mm	4.571 ± 0.451	4.754 ± 0.837
Tb.Th, mm	0.036 ± 0.004	0.032 ± 0.004
Tb.Sp, mm	0.184 ± 0.025	0.185 ± 0.043
MS/BS, %	38.70 ± 2.869	55.60 ± 4.375[a]
MAR, µm/d	2.081 ± 0.155	3.139 ± 0.175[a]
BFR/BS, $\mu m^3/\mu m^2/d$	0.808 ± 0.116	1.719 ± 0.191[a]

Mean ± SD (seven to nine mice per group).

[a] $P < .01$ vs NT.